Korean J. Chem. Eng., 33(10), 2761-2770 (2016)
DOI: 10.1007/s11814-016-0161-z
pISSN: 0256-1115
eISSN: 1975-7220

INVITED REVIEW PAPER

Flow control in paper-based microfluidic device for automatic multistep assays: A focused minireview

Seong-Geun Jeong, Jongmin Kim, Si Hyung Jin, Ki-Su Park, and Chang-Soo Lee†

Department of Chemical Engineering, Chungnam National University, Yuseong-gu, Daejeon 34134, Korea
(*Received 9 January 2016 • accepted 13 June 2016*)

Abstract−Although lateral flow tests (LFTs) are easy-to-use diagnostics, they have fundamental limitations for sequential multistep assay that can be reduced to a single chemical reaction step. Paper-based microfluidic devices have attracted considerable attention for use in automatic multi-step assays because paper can be an excellent platform to control sequential fluid flow without external equipment. This review focuses on recent developments on how to control flow rate in paper-based microfluidic devices for automating sequential multi-step assays. The aim of this review is to discuss the limitations of LFTs and potential paper-based microfluidic devices for automated sequential multi-step assays in developing countries; and the existing fluidic control technologies for sequential multi-step assays. In addition, we present future challenges for commercialization of paper-based microfluidic devices to perform automatic multi-step assays.

Keywords: Paper-based Microfluidic Device, Multistep Assays, Fluidic Time Delays, Flow Control, Diagnosis

INTRODUCTION

The traditional analytical method, lateral flow tests (LFTs), is the standard format for bioassay in developed and developing countries because it is low-cost, equipment-free, easy-to-use, rapid assay and portable [1-6]. However, LFTs often have a limitation for sequential multistep assays such as enzyme enzyme-linked immunosorbent assay (ELISA) or signal-amplified immunoassay without manually added user step. Paper-based microfluidic devices have attracted considerable attention for use in a wide range of applications for multi-step assays because they provide a portable, inexpensive, rapid assay that requires small volumes of reagents [1-18]. In particular, paper can be an excellent platform to control sequential fluid flow without external equipment [3,8,19-26]. The sequential fluid flow in the paper-based device can transfer sequentially analytes and reagents to a specific detection zone for sequential reaction. Thus, the major advantage of paper-based microfluidic devices is to carry out sequential multistep assay that cannot be performed in conventional LFTs without adding steps.

The capabilities of paper-based microfluidic devices were enhanced by two major developments in the field [26]: microfluidic paper-based analytical devices (μPADs) and paper networks (PNs). μPADs, introduced by the Whitesides group in 2008, can distribute fluids from a single inlet to multiple detection zones and can be used for simultaneous multiplex assays [26-30]. PNs, introduced by the Yager group in 2010, can be used to flow multiple fluids with a sample or reagents sequentially to a detection zone and enable performing multistep immunoassays in the devices, which go beyond the capacities of conventional lateral flow immunoassays [20,26,29,31-36].

The μPADs and PNs, can be classified into two categories, depending on the dimensions of fluid flow in devices. The first category is one-dimensional (1D) paper-based microfluidic devices, which are designed to laterally move fluid in one dimension (Fig. 1(a)) [10,37,38]. The second category is two-dimensional (2D) paper-based microfluidic devices, which are designed to horizontally move fluid in the x-y plane. (Fig. 1(d)) [30]. The third category is three-dimensional (3D) paper-based microfluidic devices, which can facilitate fluid flow in the x-y-z-direction (Fig. 1(f)) [12]. Fluid in 3D paper-based microfluidic devices can freely move in both the horizontal and vertical directions. Recently, research groups have been incorporating functionality into the paper-based microfluidic devices for better fluid handling and autonomous operation within the device, transcending traditional analytical tools [3,8,19,20,22-26,34]. In this review, we focus on recently developed methods to control flow and flow rate in paper-based microfluidic devices for automatic multistep assay. There are constraints that must be addressed when designing a device to implement multistep processes that are required to achieve obvious results of the assay in automatic operation. In addition, the device should be affordable, specific, sensitive, user-friendly, rapid and robust, equipment-free and deliverable for developing countries [8]. According to this reference, we searched and selected papers in high impact journal, relating to paper-based microfluidic device to perform automatic multistep assays in the time period from 2012 to 2015. We may have missed many outstanding papers of authors in paper microfluidic communities. In advance, we apologize to the authors. Finally, this review focuses on methods to control flow and flow rate for automating sequential multi-step assays in paper-based devices, according to 2D and 3D flow control technologies.

†To whom correspondence should be addressed.
E-mail: rhadum@cnu.ac.kr

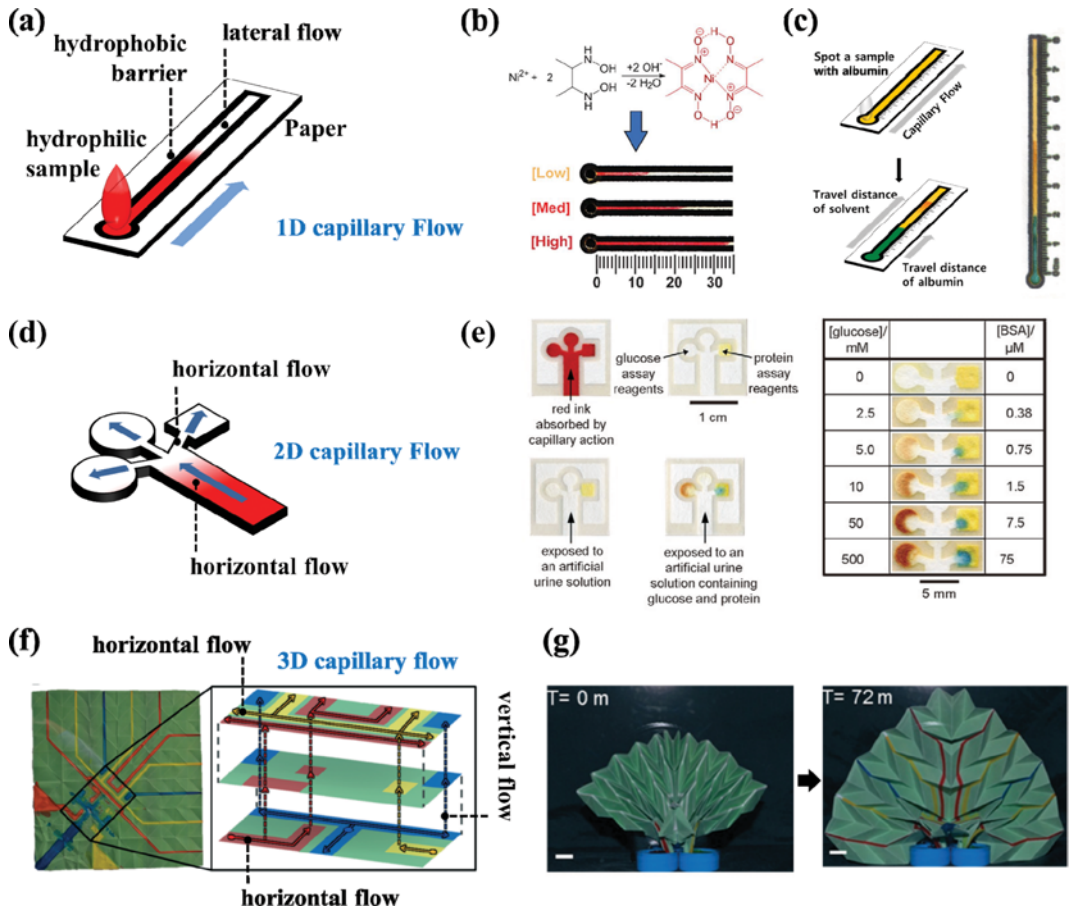

Fig. 1. Classification of paper-based microfluidic devices. (a) One-dimensional (1D) paper-based microfluidic devices, which are designed to laterally move fluid in one dimension. (b) Example of 1D devices for distance-based measurement of concentration of nickel. Copyright (2013) The Royal Society of Chemistry. (c) Example of 1D devices for ratio-based measurement of concentration of albumin. Copyright (2013) The Korean Society for Biotechnology and Bioengineering. (d) Two-dimensional (2D) paper-based microfluidic devices, which are designed to horizontally move fluid in the x-y plane. (e) Example of 2D devices for multiple detection of bovine serum albumin (BSA) and glucose. Copyright (2007) WILEY-VCH Verlag GmbH & Co. KGaA, Weinheim. (f) Three-dimensional (3D) paper-based microfluidic devices, which are designed to move horizontally and vertically flow in the x-y-z-direction. (g) Example of 3D devices for non-planar origami circuit. Copyright (2015) The Royal Society of Chemistry.

FUNDAMENTAL PHYSICS IN FLOW CONTROL

Automatic flow control in paper-based microfluidic devices is often based in controlling wicking-based flow into paper. The wicking-based flow is a process of capillary flow in porous media that can be described by Lucas-Washburn's equation [39]:

$$l(t) = \sqrt{\frac{\gamma r \cos\theta t}{2\mu}} \quad (1)$$

where $l(t)$ can be the distance traveled by fluid in paper channel, t is time, r is the average pore radius, μ is the dynamic viscosity of fluid. γ is the surface tension, θ is the contact angle. Eq. (1) often does not account for capillary flow under ambient condition since it was derived regardless of the effect gravity and evaporation. In the case of the effect of gravity on capillary flow, Rogacs et al. studied the effect of gravity on capillary flow in thin nanostructure film [40]. They found that gravity has negligible influence on vertical capillary flow in thin films. Camplisson et al. found that gravity does not significantly affect capillary flow in a paper-based channel [41]. On the other hand, Eq. (1) tends to overestimate capillary flow velocity under low humidity [41]. To improve prediction in Eq. (1), Martinez group and Stone derived a modified Lucas-Washburn equation to model capillary flow in a paper-based microfluidic device, considering loss of fluid in channel due to evaporation [42]:

$$l(t) = \sqrt{\frac{\gamma r \phi h \cos\theta t}{4\mu q_0}\left(1 - e^{-\frac{2q_0}{\phi h}t}\right)} \quad (2)$$

where h is the height of the paper-based channel, ϕ is the porosity of a paper, q_0 is evaporation rate. The Martinez group demonstrated that respective values, predicted by Eq. (2), are relatively close to values of wicking velocity in paper-based channel than Eq. (1) [42]. In this review, researchers in paper-based microfluidic community demonstrated that the capillary flow velocity can be controlled by altering the length (l), height (h), porosity (ϕ), pore radius (r) of paper channel and viscosity (μ) of fluids. Those velocity control technologies in paper-based channel allow sequential

and reaction for automatic multistep assays.

FLOW CONTROL IN TWO-DIMENSIONAL DEVICES

Recent fluidic control technology on a two-dimensional paper-based microfluidic device for automatic sequential delivery can be classified into two categories, based on the geometry and the use of chemicals [3,7,20,23,24]. First, geometry-based flow control systems are based on (1) varying the geometry of the microfluidic channel, (2) multiple volume-limited fluid sources, (3) delayed shunt, and (4) pressured paper. Second, chemical-based flow control systems are based on sugar-deposition.

1. Geometry-based Flow Control Systems

The first geometry-based flow control strategy involves changing the length of the channels. Apilux et al. used the baffle design to increase the length of the paper-based channels that allows for time delays of the sequential reagent flows to the detection region (Fig. 2(a-b)) [7]. Using this basic concept, they demonstrated paper-based devices to automate the sequential multistep reaction of enzyme-linked immunosorbent assay (ELISA). The device was fabricated with nitrocellulose (NC) membranes involving designed channels, where the reagents are deposited at specific locations for controlling the fluid travel to the detection region (Fig. 2(b)). ELISA results were accomplished in a single step. The devices performed a simple procedure to dip the input leg into sample solution for the ELISA that requires small volumes of reagents in short time. This developed device was specifically used to determine the levels of human chorionic gonadotropin (hCG) by automatic ELISA (Fig. 2(c)).

The second geometry-based flow control strategy is based on multiple volume-limited fluid sources. Fluid source pads of different sizes release a fixed volume of fluids, thereby generating sequential multiple flows to the detection region (Fig. 3(a)). Based on this concept, Fu et al. demonstrated a two-dimensional paper network (2DPN) for automatic sandwich format immunoassay including signal-amplification for the malaria protein *Pf* HRP2. Multiple inlets per detection zone in the 2DPN allow the high performance for automatic multistep processes [20]. The length of channel, from an inlet to the detection zone, decreases from left to right (Fig. 3(a)). This 2DPN topology enables the programmed delivery of first reagent A, second reagent B, and third reagent C sequentially to the detection region (Fig. 3(a-b)). They also created an easy-to-

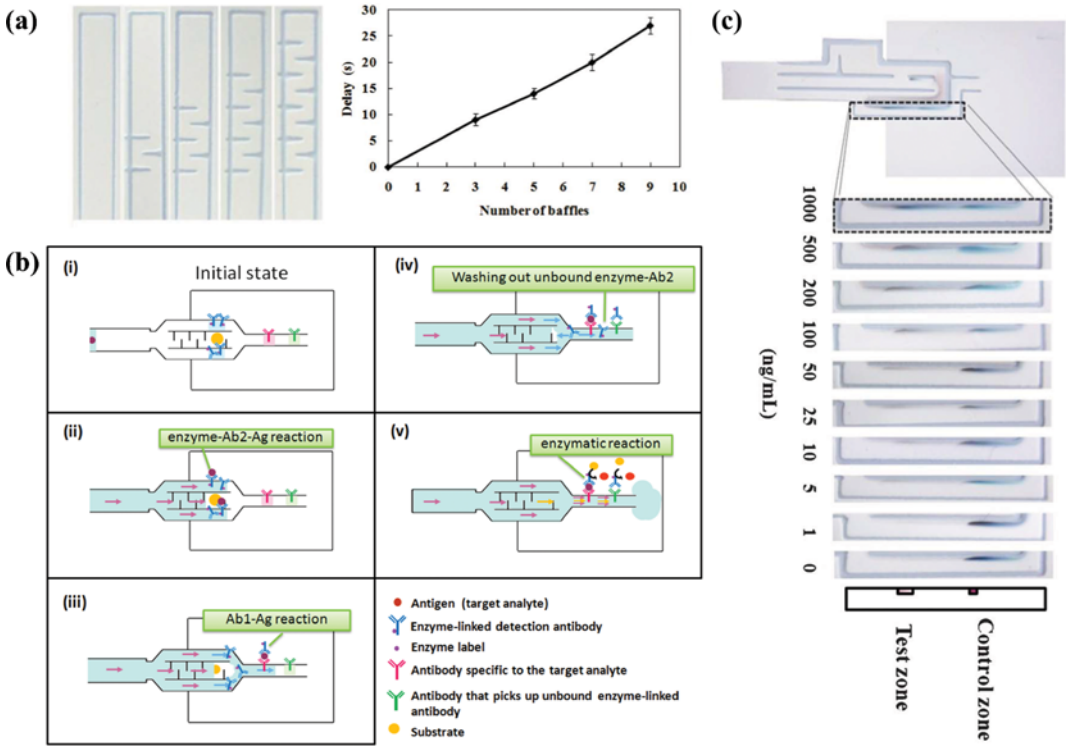

Fig. 2. Automated paper-based devices for sequential multistep sandwich enzyme-linked immunosorbent assays (ELSIA). (a) Relation between the number of baffle lines and the fluid delay. (b) Schematic of the procedure for automatic ELISA on paper-based microfluidic devices. (i) The sandwich ELISA automatically ran through the sequential reaction; (ii) the analyte solution migrated to the pre-spotted region of enzyme-Ab2 in the nondelaying channel, and the appropriate Ag(s) bound to the solubilized enzyme-Ab2 to form enzyme-Ab2-Ag complexes; (iii) the complexes were captured further along with immobilized Ab1 at the test zone; (iv) the free enzyme-Ab2 (not Ag-bound) was captured by the immobilized Ab at the control zone and washed away by sample solution; however, since some of the enzyme-Ab2-containing fluid may migrate to the delaying channel, contacting substrate containing sample fluid, color may be generated upstream of the test zone; and (v) the slower substrates migrating through the delaying channel were gradually dissolved and pass through the test zone and the control zone, allowing the enzyme reaction to occur and the color to develop (change) at the test and control zones. (c) Actual image of human chorionic gonadotropin (hCG) ELISA results on the device. Copyright (2013) The Royal Society of Chemistry.

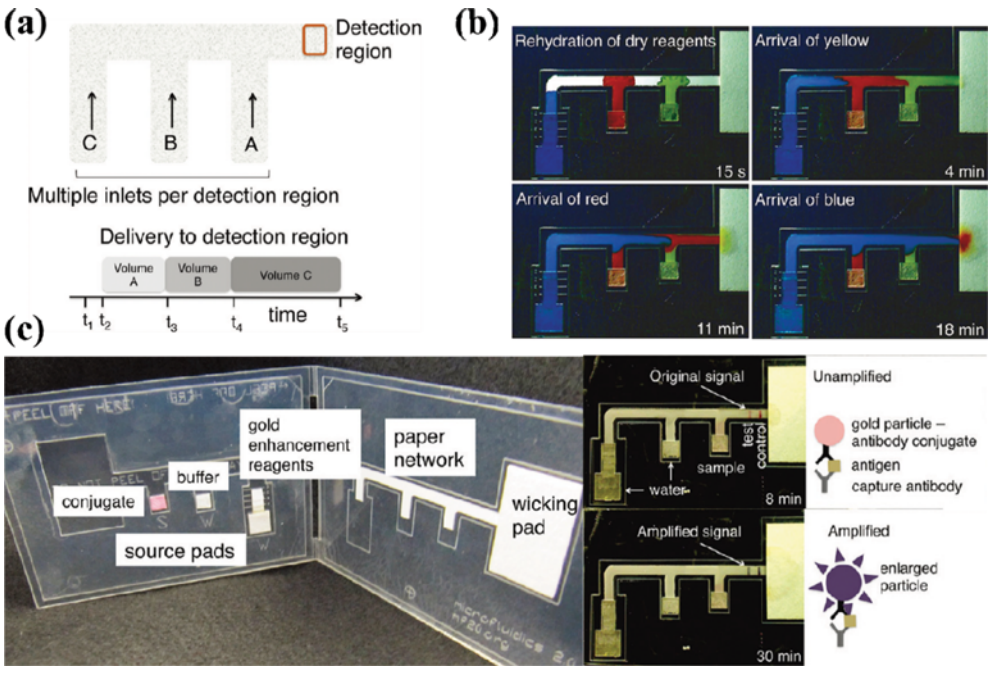

Fig. 3. Two-dimensional paper network format that enables simple multistep assays for use in low-resource settings in the context of malaria antigen detection. (a) Sequential delivery in a two-dimensional paper network (2DPN). (b) Sequential multiple flows in a 2DPN. (c) 2DPN card demonstrated for an amplified immunoassay. The results of 2DPN assay were obtained at an analyte concentration of 200 ng/mL. Copyright (2012) American Chemical Society.

use 2DPN card to store reagents in dry state; thus users need only add the sample and water for assay (Fig. 3(c)). The multiple flows in the device are activated in a single-step that users fold the card closed; the 2DPN on the card automatically delivers the suitable volumes of (1) sample with gold particle- antibody conjugate, (2) a rinse buffer solution, and (3) a gold enhancement reagent to the capture region. These results indicate the platform can be used for high-quality diagnostic capabilities in developed and developing

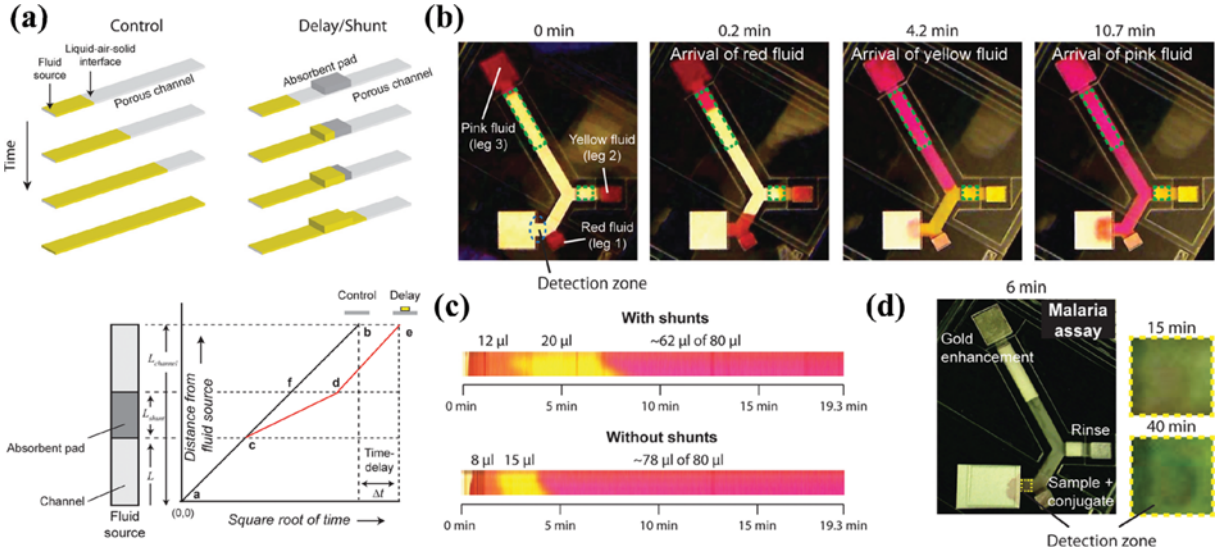

Fig. 4. Tunable-delay shunts for paper microfluidic devices. (a) Fluid delays based on absorbent pads-based shunts. (b) Time-lapse images of the sequential delivery of red, yellow, and pink fluids to a detection zone in a folding-card device. Legs 2 and 3 in the device contained absorbent pads-based shunts indicated by the dotted green lines. (c) Actual image of the detection zone, outlined by the dotted blue lines, in the folding card including shunts and not including shunts. The shunts can be used for delivery of larger volumes of fluid to the detection zone. (d) Folding card device for amplified detection of the malaria protein *Pf* HRP2. Copyright (2013) The Royal Society of Chemistry.

countries.

The third geometry-based flow control strategy is based on delay shunt. Bhushan et al. demonstrated a method to delay fluid in the porous channel by diverting fluid into an absorbent shunt placed on the channel (Fig. 4(a)) [23]. The distance traveled by the fluid front will follow the Washburn equation in the absence of the shunt, represented by a straight line on a distance versus square root of time. In the presence of the absorbent shunt, the fluid front follows also the Washburn equation before reaching the shunt. However, the absorption of fluid by the shunt slows down the movement of the fluid front in the channel after reaching the absorbent shunt. In addition, the fluid velocity increases again after the fluid front passes the shunt. The shunts provide delays, ranging from 3 min to nearly 20 min by using control of the dimensions of the absorbent pad of the shunt. In addition, an important advantage of using the absorbent shunts is to transfer larger volumes of fluids using the same (Fig. 4(b-c)). Finally, the absorbent shunts are appropriate for the sequential fluid flow to a detection zone in a point-of-care device for the amplified detection of the malaria protein P*f* HRP2 (Fig. 4(d)).

The fourth geometry-based flow control strategy is to pressurize a specific region in the paper-based channel for programmed sample delivery. Shin et al. reported a method to handle the fluid flow in porous channel simply by pressing over the specific region of porous channel surface, thereby decreasing the pore size of the porous channel [24]. As a result, permeability and fluid resistance is decreased and increased, respectively, in the pressed region and creates fluid delay (Fig. 5(a-b)). They confirmed that flow rate decreased in accordance with increased different amounts of pressure applied, up to a 740% decrease in flow velocity. In addition, they demonstrated flow rate control for sequential delivery of multiple fluid samples in a polypropylene sheet-based device that performs a multi-step colorimetric immunoassay (Fig. 5(c-e)).

2. Chemical-based Flow Control Systems

The chemical-based flow control system is based on the deposition of sugar into a paper-based channel to cause the delay of a fluid. The velocity of fluid flow can be controlled by depositing different amounts of sugar on paper-based channels [3]. The flow is blocked by solid sugar, and the flow resumes after dissolving the sugar. Lutz et al. used dissolvable sugar deposited to paper for creating programmable flow delays. They used these time delays to perform program automated multi-step assay on paper network topology. They added solutions of sucrose at different concentrations to paper strips and then dried it to create fluidic time delays (Fig. 6(a-b)). Thus, this novel PN can be used to perform automatic multi-step assays that cannot be accomplished in conventional LFTs without manually added user steps. They demonstrate a PN on folding card format, including sugar delays, to automate a four-step fluidic process by activation of a single user step (Fig. 6(c-e)). In addition, the card does not require any precise pipetting steps, such that the user steps to add uncontrolled volumes of sample solution. The device can deliver accurate volumes to each pad of the 2DPN. The folding card format can automate the pad loading step, making operation of these devices as simple as existing LFTs. They used this device to perform a sequential signal-amplified sandwich immunoassay for detection of malaria (Fig. 6(f-i)). The devices are appropriate platform for automating multistep assay that are used in multistep laboratory protocols but in an easy-to-use, rapid and inexpensive format.

FLOW CONTROL IN THREE-DIMENSIONAL DEVICE

1. Valve-based Flow Control System

Recent fluidic control methods for automatic sequential delivery in a three-dimensional (3D) paper-based microfluidic device are based on a mechanically actuated valve to connect or disconnect channels. Bhushana et al. developed a toolkit containing paper microfluidic valves and novel methods for automatic valve actuation, based on movable paper-based channels and fluid-triggered expanding components [26]. They used the valves to actuate auto-

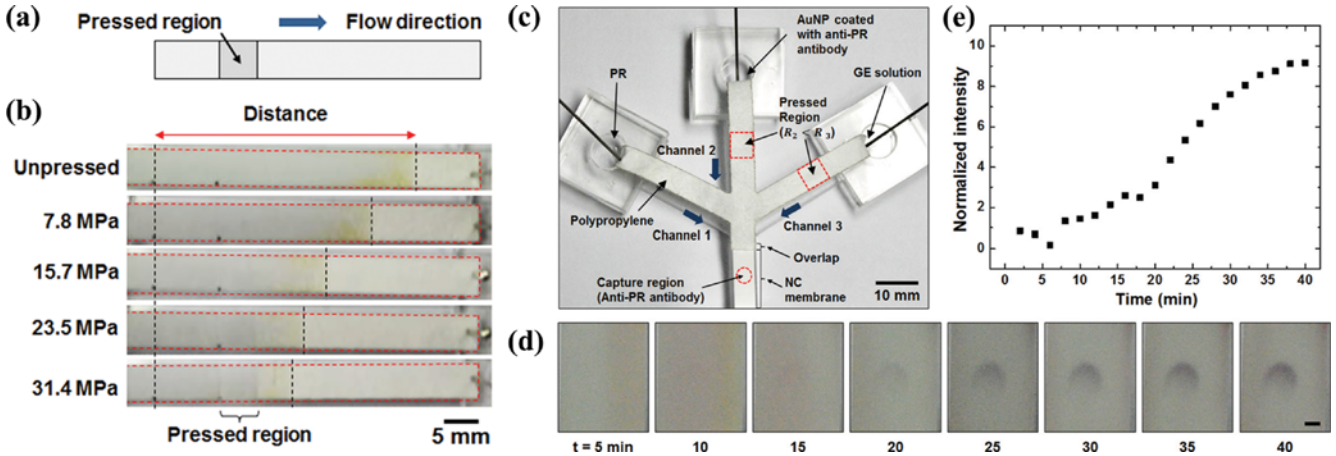

Fig. 5. Programmed sample delivery on pressurized paper. (a) Schematic of the porous channel with a specific pressed region. (b) Actual images of travel distanced by water through polypropylene sheet-based strips in accordance with increased amounts of applied pressure. (c) Design of three-branched channel for immunoassay. (d) Time-lapse images showing immunoassay results at the capture antibody region. (e) Relation between average greyscale value of colorimetric immunoassays result and time. Copyright (2014) American Institute of Physics.

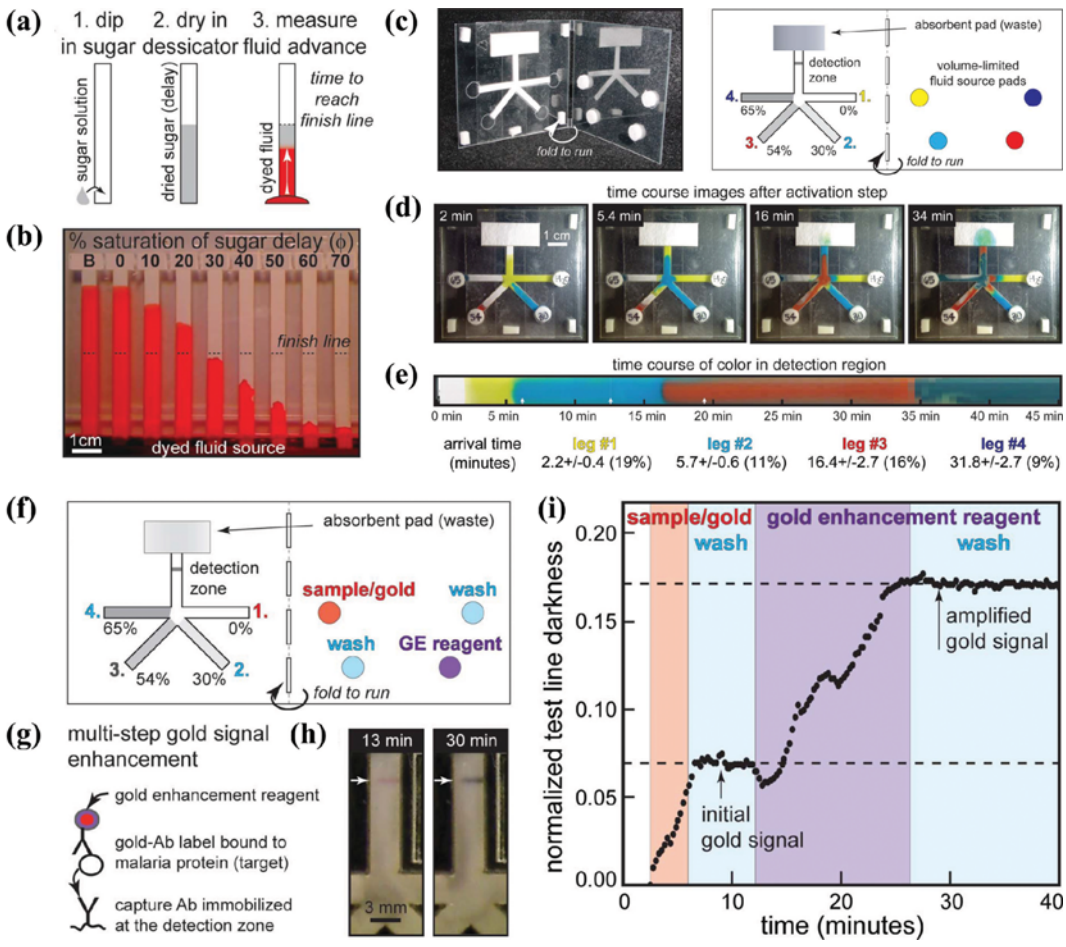

Fig. 6. Dissolvable fluidic time delays for programming multistep assays in instrument-free paper diagnostics. (a) Strategy to prepare paper strips and measure delay times. Each paper strip was dipped in a sugar solution and dried with a desiccator. (b) Actual image of paper strips deposited with different sugar solutions. (c) Design and actual image of folding card to create sequential delivery on two-dimensional paper network (2DPN) with sugar time delays. (d) Images of sequential fluid flows to the detection zone. (e) Color changes as function of time at the detection zone. (f) Card design to perform automated multi-step for detection of malaria. (g) Illustration of the signal-amplified sandwich immunoassay. (h) Actual image of the signal during the assay. (i) Time course of signal at the detection zone. Copyright (2013) The Royal Society of Chemistry.

matically after (1) a specific period of time or (2) the transit of a specific volume of fluid. The timing of valve actuation can be controlled by changing the lengths of timing wicks, and they present timed on-valves, off-valves, and diversion valves (Fig. 7(a)). These valves consist of nitrocellulose-based flow channels and glass fiber-based actuation channels. They manually add water to the glass fiber-based actuation channels after a specific period of time to actuate valves. In Fig. 8(a), A is a schematic illustration of an on-switch. A channel lifts vertically and connects to B channel after actuation. B is an actual image of yellow fluid flow in the on-switch before and after actuation. C is the velocity of the fluid front in the flow channels as a function of time. D is the schematic illustration of an off-switch containing A and B channels. The A and B channel are connected at one end. A channel lifts vertically and disconnects from B channel after actuation. E is an actual image of yellow flow in the off-switch before and after actuation. F is velocity of the fluid front in the flow channels as a function of time. G is a schematic illustration of a diversion switch. H and I are images of top and side view of the diversion-switch, respectively, before and after actuation. J is the velocity of the fluid as a function of time. Finally, they demonstrated the use of these valves in a device to perform a multi-step assay for the detection of the malaria protein (Fig. 7(b-g)). The device consists of one test strip, three source legs, one feeder channel, and one timing wick. There are three on-switches, $V_{ON,1}$, $V_{ON,2}$, $V_{ON,3}$, and an off-switch, V_{OFF}. An off-switch, V_{OFF}, disconnects the feeder channel from source legs 1, 2, and 3 after actuation. Based on the three on-switches ($V_{ON,1}$, $V_{ON,2}$, $V_{ON,3}$), three-dimensional fluid flows sequentially over the detection zone, yellow second fluid, wash third fluid, and green fourth fluid, rehydrated from legs 1, 2, and 3, respectively (Fig. 7(e-f)). This valving and automation toolkit can be used for multi-step fluidic operations on paper-based devices to demonstrate in the malaria assay device. In Fig. 7(g), the two spots indicate the test result and control.

2. 3D Microfluidic Network-based Flow Control System

3D paper-based microfluidic device can move complex fluid through the thickness of paper (the z-direction) and horizontally

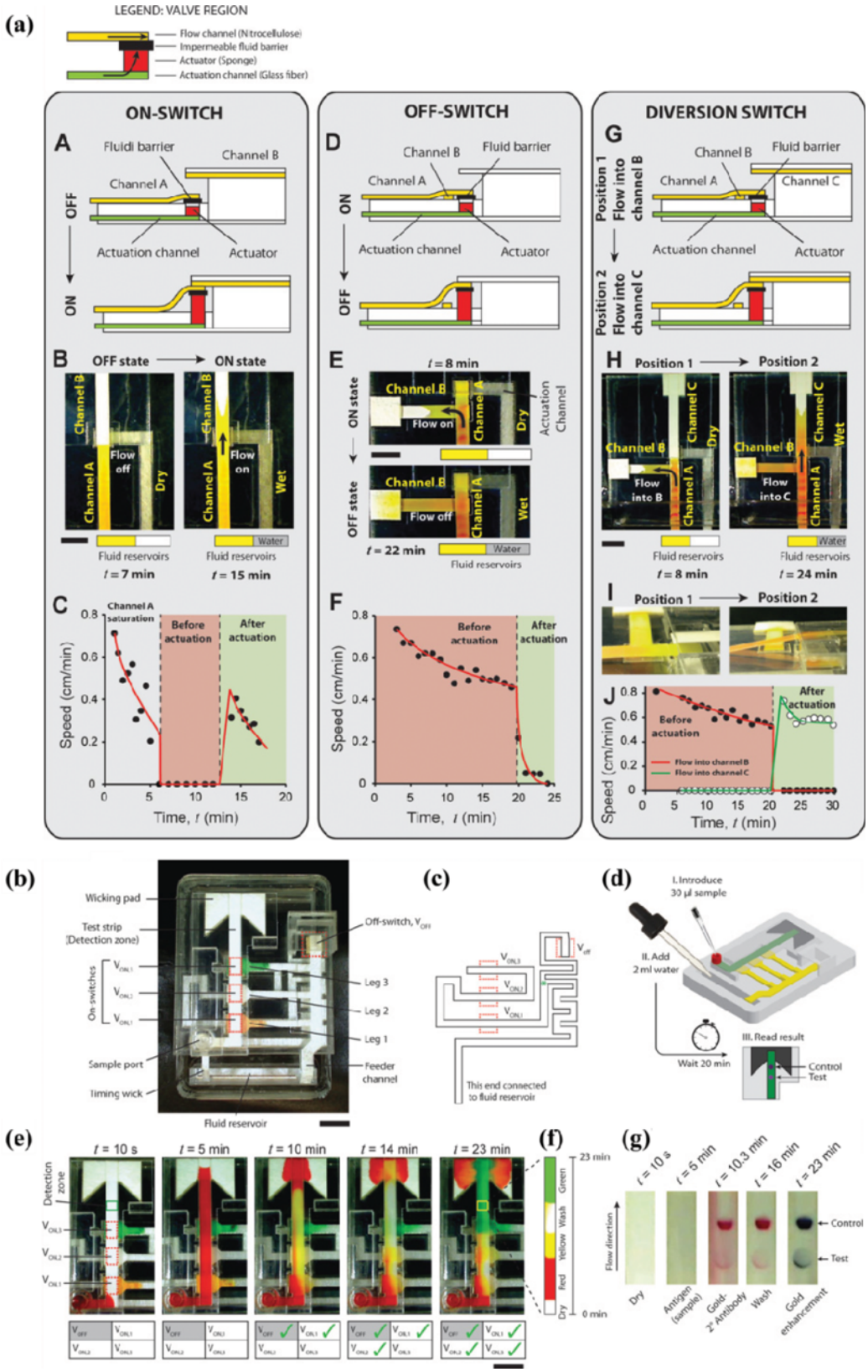

Fig. 7. A versatile valving toolkit for automating fluidic operations in paper microfluidic devices. (a) The three types of time-metered valves: (1) A, B, C are on-switches, (2) D, E, F are off-switches and (3) G, H, J are diversion switches. (b) Top view of the malaria protein detection device. (c) The design of the timing wick and the four valves. (d) Schematic of a step-by-step procedure for protein detection test. (e) Colored fluid flow in the automatic operation. (f) Time-lapse images of detection zone at 23 min. (g) Time course of the detection zone of the device to perform multi-step protein detection assay. Copyright (2015) The Royal Society of Chemistry.

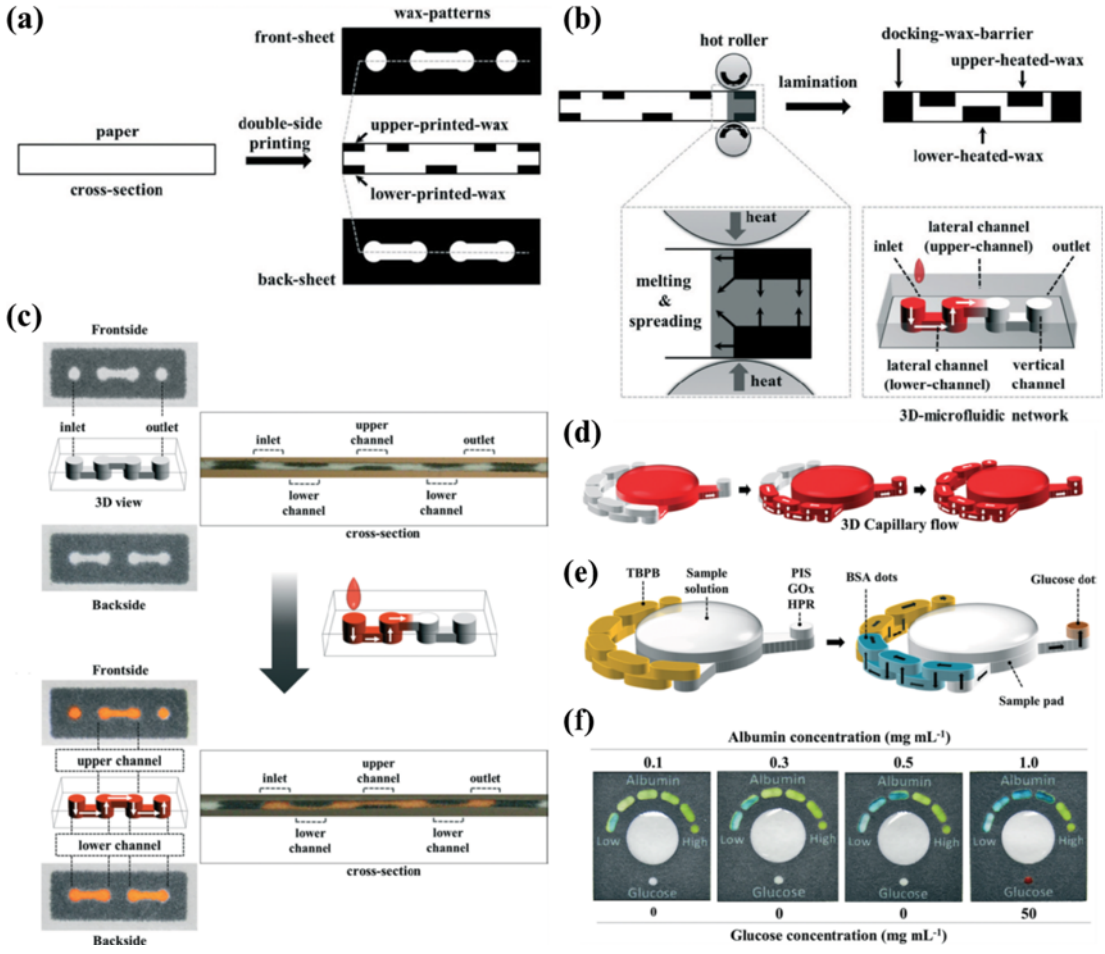

Fig. 8. Single sheet of three-dimensional microfluidic device to control movement of capillary flow in x-y-z direction. The 3D device is fabricated by double-sided printing and lamination. (a) Double-sided printing: a wax printer prints the wax patterns on both sides of a paper. (b) Lamination: two hot rollers in a laminator melt the wax patterns, and the heating time can be controlled by altering the rotation rate of the hot rollers. (c) Demonstration of a 3D capillary flow in a paper. (d) Illustration of 3D flow in the device for digital assay. (e) Functionalization by wicking with tetrabromophenol blue (TBPB), potassium iodide (PI), glucose oxidase (GOx), and horseradish peroxidase (HPR). (f) Digital assay after the introduction of a sample solution with albumin or glucose. The number of blue colored dots increased depending on concentration of albumin in the sample. The colorless glucose dot also changed color to brown when glucose was present. Copyright (2015) The Royal Society of Chemistry.

(the x-y-plane) for multiplex and digital assay in 3D microfluidic network. Our group demonstrated a simple approach for fabricating a 3D paper-based microfluidic device from a paper by double-sided printing and lamination (Fig. 8) [12]. First, a wax printer prints vertically symmetrical and asymmetrical wax patterns on the surface of both-sided paper (Fig. 8(a)). Second, a laminator melts the wax on the paper, then the melted wax penetrates into a paper to form 3D microfluidic channels in a paper (Fig. 8(b)). The vertically symmetrical wax pattern forms vertical channels when the melted wax contact with each other. The asymmetrical wax pattern forms lateral and vertical channels when the wax penetrates to a lower height than the thickness of paper. Finally, the two types of wax patterns form a 3D microfluidic network to move fluid horizontally and vertically in the thickness of a paper. Our group demonstrated the ability of 3D channel to move fluids in 3D-space (Fig. 8(c)). When a red dye solution was introduced into the inlet, the solution flowed horizontally and vertically from the inlet to the outlet through the 3D microfluidic network (Fig. 4(c)). The docking wax barrier prevented fluid from leaking out and formed the inlet and the outlet in the thickness of paper. The lower and upper channels guided the horizontal flow, while the vertical channels induced vertical fluid flow. Based on this concept, our group created a digital assay of albumin in the 3D device without using an external detection apparatus. The 3D device distributes the sample from the single sample pad to the BSA and glucose dots (Fig. 8(d-f)). For albumin assay, citrate buffer solution is spotted on BSA dots and then layered tetrabromophenol blue (TBPB) since the color of TBPB changes from yellow to blue when it ionizes and binds to albumin. [30] For glucose assay, glucose oxidase, horseradish peroxidase, and potassium iodide were adsorbed in the glucose dot. The reagents were allowed to air dry at room temperature. In this 3D device, assay protocol is accomplished by one-step to drop sample solution on sample pad. Sample was divided into two flows toward the BSA and glucose dots.

First, while the sample flowed from the sample pad to the BSA dots, the yellow colored TBPB in the BSA dots changed to blue via reaction with albumin. Flowing the sample through 3D microfluidic network allowed for a consecutive color change as albumin molecules were consumed by reaction with TBPB. Thus, our group can easily measure the concentration of the albumin by simply counting the number of colored dots. This assay provides a novel format for digital diagnostics to indicate the amount of albumin. Second, the sample also flowed from the sample pad to the glucose dot. The color of potassium iodide in the glucose dot is changed to a brown color in the presence of glucose. In the case of a sample with albumin and glucose, the device clearly indicated four blue dots and a red glucose dot (Fig. 8(f)). This result shows that the 3D device can simultaneously perform multiple diagnostic assays under this novel format of digital diagnostics.

CONCLUSION AND FUTURE DIRECTION

The recently reported paper-based microfluidic devices are inexpensive, equipment-free, portable, and user-friendly. In particular, the devices have several unique benefits for automatic multi-step assay: (1) minimization of the number of required user steps, (2) stable storage of dry reagents within the devices in changing environments, (3) improvement of assay sensitivity, transcending traditional LFTs, by incorporating additional assays steps, (4) minimization of amount of reagents required to achieve the same level of performance. Importantly, the flow control strategies in this review provide fluidic time delay on paper channels as enough as to perform sequential fluidic process for high performance application such as enzyme-linked immune assay or signal-amplified immunoassay (Table 1). However, the reported geometrical or chemical treatment based strategies have a limitation for rapid production due to specific process such as assembly, deposition sugar, bridge formation for about 48 hours. Valve-based strategy is an easy-to-use and powerful method to perform automatic multistep assay, but requires multiple steps for fabrication, stacking, mounting and connection. The limitations may lead to fail roll-to-roll manufacturing, which are more efficient for commercial-scale manufacturing. In developing countries' markets, some devices for multistep assay may be found, but the World Health Organization (WHO), as well as governmental agencies, look for an adequate price that can be accepted by the users [8,26]. Therefore, commercial-scale manufacturing considerations are essential to achieve developing world markets penetration.

ACKNOWLEDGEMENTS

This work was supported by the Global Research Laboratory (NRF-2015K1A1A2033054) through the National Research Foundation of Korea (NRF) funded by the Ministry of Science, ICT (Information and Communication Technologies) and Future Planning. This study was supported by a grant from the National Research Foundation of Korea (NRF), funded by the Korean government (MEST) (no. 2011-0017322). This study was supported by the research fund of Chungnam National University (2016).

REFERENCES

1. G. Posthuma-Trumpie, J. Korf and A. van Amerongen, *Anal. Bioanal. Chem.*, **393**, 569 (2009).
2. S. Haeberle and R. Zengerle, *Lab Chip*, **7**, 1094 (2007).
3. B. Lutz, T. Liang, E. Fu, S. Ramachandran, P. Kauffman and P. Yager, *Lab Chip*, **13**, 2840 (2013).
4. D. Mark, S. Haeberle, G. Roth, F. von Stetten and R. Zengerle, *Chem. Soc. Rev.*, **39**, 1153 (2010).
5. B. Ngom, Y. Guo, X. Wang and D. Bi, *Anal. Bioanal. Chem.*, **397**, 1113 (2010).
6. B. Weigl, G. Domingo, P. LaBarre and J. Gerlach, *Lab Chip*, **8**, 1999 (2008).
7. G. M. Whitesides, *Lab Chip*, **13**, 4004 (2013).
8. G. E. Fridley, H. Le and P. Yager, *Anal. Chem.*, **86**, 6447 (2014).
9. C.-M. Cheng, A. W. Martinez, J. Gong, C. R. Mace, S. T. Phillips, E. Carrilho, K. A. Mirica and G. M. Whitesides, *Angew. Chem. Int. Edi.*, **49**, 4771 (2010).
10. D. M. Cate, W. Dungchai, J. C. Cunningham, J. Volckens and C. S. Henry, *Lab Chip*, **13**, 2397 (2013).
11. D. M. Cate, S. D. Noblitt, J. Volckens and C. S. Henry, *Lab Chip*, **15**, 2808 (2015).
12. S.-G. Jeong, S.-H. Lee, C.-H. Choi, J. Kim and C.-S. Lee, *Lab Chip*, **15**, 1188 (2015).
13. J. L. Osborn, B. Lutz, E. Fu, P. Kauffman, D. Y. Stevens and P. Yager, *Lab Chip*, **10**, 2659 (2010).
14. B. Kalish and H. Tsutsui, *Lab Chip*, **14**, 4354 (2014).
15. M. Ariza-Avidad, A. Salinas-Castillo and L. F. Capitán-Vallvey, *Biosens. Bioelectron.*, **77**, 51 (2016).
16. L. F. Capitán-Vallvey, N. López-Ruiz, A. Martínez-Olmos, M. M. Erenas and A. J. Palma, *Ana. Chim. Acta*, **899**, 23 (2015).
17. S.-A. Im, W. Wang, C.-K. Lee and Y. N. Lee, *Immune Netw.*, **10**, 230 (2010).

Table 1. Flow control in paper-based microfluidic device for automatic multistep assay

Classification	Controlling strategy	Major component	Application	Reference
2D flow control	Geometry	Baffled or teared channel	Enzyme-linked immunosorbent assay	[7,43,44]
	Geometry	Multi limited-volume source	Enzyme-linked immunosorbent assay	[8,20,21]
	Geometry	Delayed absorbent shunt	Signal-amplified immunoassay	[23,33,35]
	Geometry	Pressurized or crafted paper	Signal-amplified immunoassay	[24,45,48]
	Chemical treatment	Sugar deposition	Signal-amplified immunoassay	[3,22,46]
3D flow control	Valve	Fluid-triggered valve	Signal-amplified immunoassay	[26,47]
	Geometry	3D microfluidic network	Protein and enzymatic glucose assay	[12,38]

18. K. H. Kim, *Int. Neurourol J.*, **17**, 153 (2013).
19. A. Apilux, Y. Ukita, M. Chikae, O. Chailapakul and Y. Takamura, *Lab Chip*, **13**, 126 (2013).
20. E. Fu, T. Liang, P. Spicar-Mihalic, J. Houghtaling, S. Ramachandran and P. Yager, *Anal. Chem.*, **84**, 4574 (2012).
21. E. Fu, P. Kauffman, B. Lutz and P. Yager, *Sens. Actuators, B: Chem.*, **149**, 325 (2010).
22. S. Jahanshahi-Anbuhi, A. Henry, V. Leung, C. Sicard, K. Pennings, R. Pelton, J. D. Brennan and C. D. M. Filipe, *Lab Chip*, **14**, 229 (2014).
23. B. J. Toley, B. McKenzie, T. Liang, J. R. Buser, P. Yager and E. Fu, *Anal. Chem.*, **85**, 11545 (2013).
24. J. H. Shin, J. Park, S. H. Kim and J.-K. Park, *Biomicrofluidics*, **8**, 054121 (2014).
25. H. Chen, J. Cogswell, C. Anagnostopoulos and M. Faghri, *Lab Chip*, **12**, 2909 (2012).
26. B. J. Toley, J. A. Wang, M. Gupta, J. R. Buser, L. K. Lafleur, B. R. Lutz, E. Fu and P. Yager, *Lab Chip*, **15**, 1432 (2015).
27. A. W. Martinez, S. T. Phillips, Z. Nie, C.-M. Cheng, E. Carrilho, B. J. Wiley and G. M. Whitesides, *Lab Chip*, **10**, 2499 (2010).
28. A. W. Martinez, S. T. Phillips and G. M. Whitesides, *Proc. Natl. Acad. Sci.*, **105**, 19606 (2008).
29. A. W. Martinez, S. T. Phillips, G. M. Whitesides and E. Carrilho, *Anal. Chem.*, **82**, 3 (2010).
30. A. W. Martinez, S. T. Phillips, M. J. Butte and G. M. Whitesides, *Angew. Chem. Int. Ed.*, **46**, 1318 (2007).
31. E. Fu, S. A. Ramsey, P. Kauffman, B. Lutz and P. Yager, *Microfluid. Nanofluid.*, **10**, 29 (2011).
32. B. R. Lutz, P. Trinh, C. Ball, E. Fu and P. Yager, *Lab Chip*, **11**, 4274 (2011).
33. E. Fu, T. Liang, J. Houghtaling, S. Ramachandran, S. A. Ramsey, B. Lutz and P. Yager, *Anal. Chem.*, **83**, 7941 (2011).
34. E. Fu, P. Kauffman, B. Lutz and P. Yager, *Sens. Actuators, B: Chem.*, **149**, 325 (2010).
35. P. Kauffman, E. Fu, B. Lutz and P. Yager, *Lab Chip*, **10**, 2614 (2010).
36. E. Fu, B. Lutz, P. Kauffman and P. Yager, *Lab Chip*, **10**, 918 (2010).
37. S.-G. Jeong, S.-H. Lee and C.-S. Lee, *Korean Soc. Biotechnol. Bioeng. J.*, **28**, 254 (2013).
38. S.-G. Jeong, J. Kim, J.-O. Nam, Y. S. Song and C.-S. Lee, *Int. Neurourol. J.*, **17**, 155 (2013).
39. E. W. Washburn, *Phys. Rev.*, **17**, 273 (1921).
40. A. Rogacs, J. E. Steinbrenner, J. A. Rowlette, J. M. Weisse, X. L. Zheng and K. E. Goodson, *J. Colloid Interface Sci.*, **349**, 354 (2010).
41. C. K. Camplisson, K. M. Schilling, W. L. Pedrotti, H. A. Stone and A. W. Martinez, *Lab Chip*, **15**, 4461 (2015).
42. E. Carrilho, A. W. Martinez and G. M. Whitesides, *Anal. Chem.*, **81**, 7091 (2013).
43. D. L. Giokas, G. Z. Tsogas and A. G. Vlessidis, *Lab Chip*, **15**, 3006 (2015).
44. K. Kerman, N. Nagatani, M. Chikae, T. Yuhi, Y. Takamura and E. Tamiy, *Anal. Chem.*, **78**, 5612 (2006).
45. I. Jang and S. Song, *Anal. Chem.*, **15**, 3405 (2015).
46. J. Houghtaling, T. Liang, G. Thiessen and E. Fu, *Anal. Chem.*, **85**, 11201 (2013).
47. X. Li, P. Zwanenburga and X. Liu, *Lab Chip*, **13**, 2609 (2013).
48. D. L. Giokas, G. Z. Tsogas and A. G. Vlessidis, *Anal. Chem.*, **86**, 6447 (2014).
49. B. Kalisha and H. Tsutsui, *Lab Chip*, **14**, 4354 (2014).

Chang-Soo Lee is a Professor in the Chemical Engineering at Chungnam Naional University in Korea. He received his B.S. degree (Inha University, Korea) in Chemical Engineering and Biological Engineering, M.S. degree (Inha University, Korea) in Biological Engineering, and Ph.D. degree (Seoul National University, Korea) in Chemical Engineering. He was a postdoctoral fellow at the M.I.T. (Massachusetts Institute of Technology, U.S.A.). He worked for three years at Honam Petrochemical R&D Center from 1996 to 1999. He was a visiting professor at Harvard University at United States of America. His research interests include Microfluidics, Lab on a Chip, High Throughput screening, Paper chip, BioSensor, Colloid.